TECHNO-ECONOMIC ANALYSIS OF AN INDIRECTLY HEATED MOVING BED REACTOR BASED THERMOCHEMICAL HEAT STORAGE AND UPGRADE SYSTEM UNDER STEADY STATE CONDITION

Dhivakaran Jayakumar[a]*, Alper Can Ince[a], Lasse Røngaard Clausen[a], Ahmad Arabkoohsar[a]

[a]Technical University of Denmark, DTU Construct-Thermal Energy Section, Department of Civil and Mechanical Engineering, Nils Koppels Allé, 2800 kgs.Lyngby, Denmark

Abstract:

Industrial sector is responsible for around 14.2 % of greenhouse gas emission (GHG) in 2023. Industrial process heat above 500 °C accounts for nearly half of the sector's total energy demand and associated greenhouse gas emissions. In addition, emits a massive amount of high temperature heat in the form of waste heat which could be utilized for other processes or onsite use after upgrading. This paper investigates a calcium hydroxide-based thermochemical heat upgrade/storage system, part of the STOREDGE project, which recovers waste heat from 400 °C and upgrades it to 600 °C via reversible solid-gas chemical reactions. The system delivers 2 MW of heat with a coefficient of performance of heating (COP_h) of 0.61, requiring 5256 kg of $Ca(OH)_2$ and a reactor volume of 7.96 m³. A detailed techno-economic assessment shows a Levelized Cost of Heat (LCoH) of 7.71 c€/kWh, with the reactor contributing 39% of total system cost and heat exchangers nearly 30%. Parametric study reveals that LCoH is highly sensitive to waste heat price (ranging from 1.2 to 13.8 c€/kWh for waste heat price 0–0.05 €/kWh) and system capacity (LCoH drops 20% from 0.5 to 50 MW) but is largely unaffected by dehydration or hydration pressure variations. Free waste heat enables LCoH below 3–4 c€/kWh, making the system competitive with natural gas boilers and industrial heat pumps.

Keywords:

Thermochemical heat storage/upgrade system; Heat recovery; High-temperature process heat; Levelized Cost of Heat

1. Introduction

The share of renewables in electricity generation has to rise by 60 % within 2030 to meet Net zero emission (NZE) by 2050 [1] . Emissions from the electricity & heat producers and industrial sector accounts for approximately 44 % and 17.8 % of total CO_2 emissions, respectively, in 2023 [2]. The emissions primarily arise from the burning of fossil fuels to generate process heat for high-temperature industrial applications such as iron and steel production, paper manufacturing, chemical processing and power generation. Therefore, the decarbonization of the industrial process heat, particularly the processes requiring heat above 500 °C is crucial, as it accounts for almost half of the total heat demand in the sector. In addition, such industries emit massive amounts of high temperature heat in the form of waste heat which could be utilized for other processes or onsite use after upgrading. Thermochemical heat storage/upgrade system is one of the technologies that shows potential for recovering and storing heat (waste heat from the industrial processes, solar thermal, excess electricity) and upgrading it to higher temperatures. This technology works based on reversible dehydration and hydration chemical reactions (endothermic/exothermic processes) of certain materials.

Several numerical and experimental studies on the thermochemical heat storage system are available. Schaube et al. [3], studied the physical properties of reactant material $Ca(OH)_2/CaO$, such as heat capacity, thermodynamic equilibrium, reaction enthalpy and reaction kinetics for both hydration and dehydration reaction process in a thermochemical heat storage system. Pardo et al. [3], reviewed the numerical, experimental and technological studies on the chemical reaction-based heat storage system (thermochemical heat storage). Schmidt et al. [5], designed an indirectly heated fixed bed reactor and conducted experimental studies on the $Ca(OH)_2$ system, and addressed the limitation in the heat and mass transfer on the charging and discharging

characteristics for the reactor. Mejia et al. [6], developed a moving bed reactor and conducted experimental studies on the reaction performance, cycling stability, flowability of the $Ca(OH)_2$ based system with coated granules to enhance the thermal conductivity. Wang et al. [7], developed a 3D Multiphysics coupled model of a shell and tube fixed bed thermochemical energy storage (TCES) for a $Ca(OH)_2$/CaO system to analyse the effect of heat transfer fluid flow direction and reactor structure on the heat transfer and reaction kinetics of the system. Jia et al. [8], reviewed the physical properties, chemical characteristics, cyclic stability, and state-of-the-art applications of a $Ca(OH)_2$ based thermochemical heat storage system.

In addition, several studies focused on the techno-economic performance of the TCES. Michalski et al. [9], studied the economic viability of calcium looping combustion-based technology for low-carbon power generation and compared the net present value with other power generation technologies such as conventional steam cycle and supercritical CO_2. Carro et al. [10], designed and evaluated a large-scale thermochemical energy storage system based on calcium hydroxide for solar thermal applications. The study assessed the technical challenges of the system operating at high temperature conditions and system economic viability. Vecchi et al. [11], assessed the techno-economic performance of various thermo-mechanical energy storage systems for long-duration energy storage targets, study includes adiabatic compressed air energy storage and thermochemical concepts. Rahbari et al. [12], assessed the technical and economic performance for a Hydration heat transformer using $SrBr_2 \cdot H_2O$ as the reactive material for an operating condition of 150–250 °C, designed to recover and upgrade low-grade industrial waste heat to high-temperature sustainable process heat.

Although several studies have examined the technical and economic performance of TCES system, detailed study on technical and economic assessment of individual system components such as reactors, heat exchangers, storage tanks, and the integrated systems is limited. Therefore, this study presents a comprehensive preliminary techno-economic assessment of both the individual system components and the integrated system. In addition, the techno-economic assessment includes a parametric study on the components' cost inputs to evaluate the influence on overall system viability. Furthermore, the influence of reaction-gas partial pressure (dehydration pressure, hydration pressure) on the heat transfer area, reactor temperature, Coefficient of Performance (COP) and Levelized Cost of Heat (LCoH) is examined.

2. Methodology

This section presents the detailed description of system design parameters, modelling assumptions, energy and economic models for the proposed system.

2.1. System description

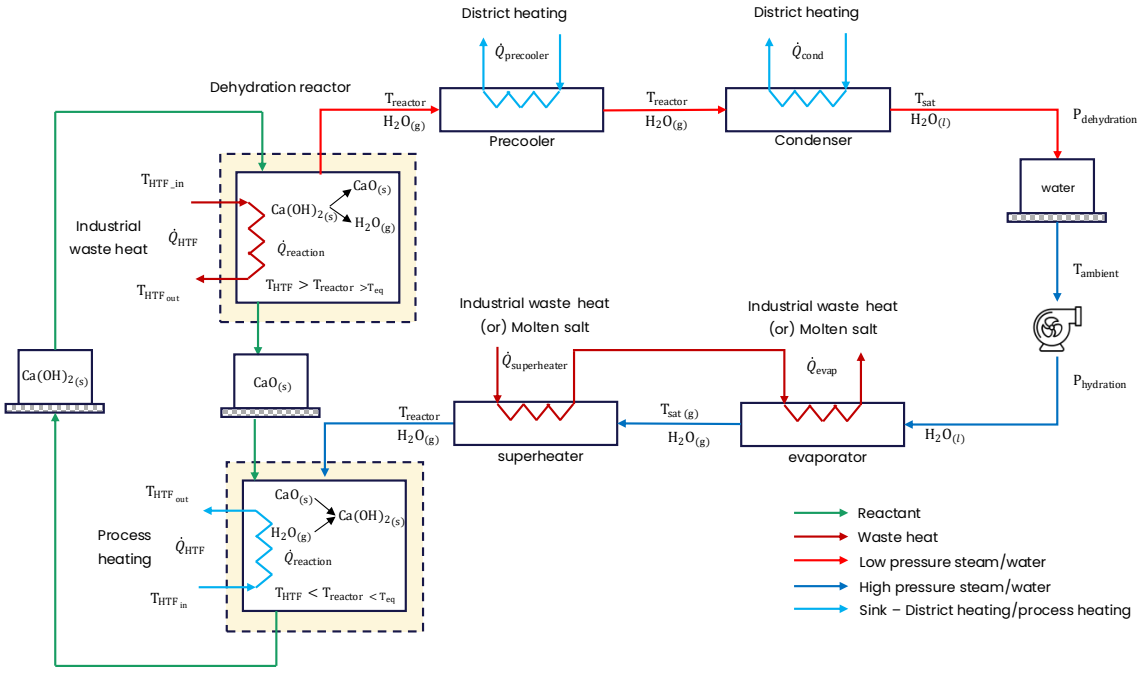

***Figure 1**. Schematic of the proposed Thermochemical heat storage system*

The schematic of the proposed indirectly heated calcium hydroxide based TCES system is shown in Figure 1. The system works based on a closed loop reversible solid-gas reaction $Ca(OH)_{2(s)} + \Delta H_{reaction} \leftrightarrow$

$CaO_{(s)} + H_2O_{(g)}$. The system consists of six major components such as dehydration reactor, hydration reactor, condenser, evaporator, storage tanks, and pump. An indirectly heated moving bed reactor is chosen for both the dehydration and hydration reactor. $Ca(OH)_2/CaO$ is chosen as reactive material pair. The system operates based on the following conditions: During the charging process, the $Ca(OH)_{2(s)}$ material filled inside the dehydration reactor absorbs heat (endothermic process) from the external heat transfer fluid and decomposes into $CaO_{(s)}$ and $H_2O_{(g)}$. Over the conversion of the material the $H_2O_{(g)}$ released is continuously removed from the reactor (as accumulation of H_2O inside the reactor increase the partial pressure and therefore increases the equilibrium pressure) before being cooled and condensed by passing through the precooler and condenser and later stored inside storage tank, while the converted $CaO_{(s)}$ is stored in storage tank.

During the discharge process, the $CaO_{(s)}$ stored in the storage tank is supplied inside the hydration reactor and reacts with the $H_2O_{(g)}$ and releases heat upon reaction (exothermic process) which is absorbed by the external heat transfer fluid. The required H_2O for the conversion of material into $Ca(OH)_{2(s)}$ is supplied from the tank, the pump supplies the pressurised water (hydration pressure), which is later evaporated and superheated to higher temperatures before entering the hydration reactor. The system can be used either as storage or heat upgrade system, depending on the operating condition (pressure levels). In the analysis, the system is assumed to be in continuous operation, meaning simultaneous operation of dehydration and hydration takes place. Therefore, the material converted inside the dehydration reactor $CaO_{(s)}$ is transferred into the hydration reactor and converted back into $Ca(OH)_{2(s)}$. Assuming continuous addition and removal of heat from the system.

2.2. Techno-economic modelling

In the analysis, the following assumptions were considered: 1) The temperature inside the reactor is assumed to be uniform. 2) The heat loss from the system to the surroundings is neglected, also pressure loss in the system components are neglected. 3) The heat supplied or absorbed by the external heat transfer fluid (waste heat) is assumed to be equal to the reaction heat required for dehydration or released during hydration reaction respectively. 4) Fixed overall heat transfers coefficients (*U*-values) are used for the heat exchangers according to type of heat transfer medium such as fluid-fluid, gas-fluid, fluid-gas. The following governing equations are used for techno-economic modelling. 5) The degradation of the material due to continuous cyclic operation inside the reactor is neglected. But, to account this effects in simplified the model, it is assumed that the material is replaced once every year.

The heat of reaction for dehydration process and hydration process is estimated by Eq. (1),

$$\dot{Q}_{\text{reaction}} = \pm\, \dot{m}_{\text{w}} \times\, \Delta \text{H}_{\text{reaction}} \tag{1}$$

Where, $\dot{m}_{\text{w}}$ is the mass flow rate of water, $\Delta \text{H}_{\text{reaction}}$ is the enthalpy of reaction.

The equilibrium temperature is estimated by the equation of Samms and Evans [13],

$$ln\left(\left(\text{P}_{\text{H}_2\text{O}}\right)[bar]\right) = -\frac{11375}{\text{T}_{\text{eq}}[K]} + 14.574 \tag{2}$$

Where, T_{eq} is the equilibrium temperature in K.

The reactor temperatures are estimated by Eq. (3), (4)

$$\text{T}_{\text{dehydration reactor}} = \text{T}_{\text{eq}} + 10\ \text{K} \tag{3}$$

$$\text{T}_{\text{hydration reactor}} = \text{T}_{\text{eq}} - 10\ \text{K} \tag{4}$$

The heat transfer area of heat exchanger is estimated by Eq. (5),

$$\dot{\text{Q}} = U \times \text{A} \times \text{LMTD} \tag{5}$$

Where, $\dot{\text{Q}}$ is the heat transfer rate, U is the overall heat transfer coefficient, A is the heat transfer area, and LMTD is the log mean temperature difference.

The pump power required to increase the water pressure to hydration pressure is estimated by Eq. (6)

$$\dot{W}_{\text{p}} = \dot{m}_{\text{w}} \times \frac{1}{\rho_{\text{w}}} \times (\text{P}_{\text{storage}} - \text{P}_{\text{hydration}}) \tag{6}$$

The volume of the reactor is estimated by Eq. (7),

$$V_{\text{reactor}} = \frac{\text{total mass of } \mathrm{Ca(OH)_2}}{\rho_{\text{bulk}}\,(1-\varepsilon)} \tag{7}$$

Where, ρ_{bulk} is the density of the material bulk, ε is the porosity of the material.

The total mass of the $\mathrm{Ca(OH)_2}$ required is estimated by Eq. (10),

$$\dot{n}_{\text{water}} = \frac{\dot{m}_{\text{w}}}{\mathrm{MW}_{\text{water}}} \tag{8}$$

Where, $\dot{n}_{\text{water}}$ is the molar flow rate of water, $\mathrm{MW}_{\text{water}}$ is the mole mass of water. According to stoichiometric condition 1:1:1,

$$\dot{m}_{\mathrm{Ca(OH)_2}} = \dot{n}_{\text{water}} \times \mathrm{MW}_{\mathrm{Ca(OH)_2}} \tag{9}$$

$$\text{total mass of } \mathrm{Ca(OH)_2} = \dot{m}_{\mathrm{Ca(OH)_2}} \times \text{time preiod of each cycle} \tag{10}$$

where, the time taken for complete conversion of each cycle is assumed to be 1 hours [12].

The total mass of CaO is estimated by Eq. (11),

$$\text{total mass of CaO} = \dot{m}_{\text{Cao}} \times \text{time preiod of each cycle} \tag{11}$$

The Coefficient of Performance of heating for the system is given by Eq. (12),

$$\mathrm{COP_h} = \frac{\dot{\mathrm{Q}}_{\text{hydration}}}{\dot{\mathrm{Q}}_{\text{dehydration}} + \dot{\mathrm{Q}}_{\text{evaporator}} + \dot{\mathrm{Q}}_{\text{superheater}}} \tag{12}$$

The material properties of the solid-gas reactant are as follows: the mole mass of water is 0.018 kg.mol^{-1}, mole mass of $Ca(OH)_2$ is 0.074 kg.mol^{-1}, mole mass of CaO is 0.056 kg.mol^{-1}, Density of $Ca(OH)_2$ is 2200 kg.m^{-3}, Density of CaO is 3320kg.m^{-3} and the Porosity of reactant is 0.7 according to [14], [7].

The economic performance of the system is estimated by the Levelized Cost of Heat. Cost functions are used to estimate the component cost of reactor, condenser, evaporator, pump and storage tank. The cost function used is given in Table 1, and the coefficients used for cost function are given in Table 2. The assumption used for the economic analysis are as follows: 1) The system lifetime is assumed as 20 years, 2) Discount rate as 5 %, 3) Maintenance cost is assumed as 5 % of capital cost, 4) Total operating hours of 8760 hours, 4) $Ca(OH)_2$ price is 70 €/kg [25], 5) Waste heat price is 30 €/MWh [22].

Table 1. *Component cost function*

Component	Cost function	Reference
Reactor	$C_{\text{reactor}} = 4.57\times10^4\times(V_{\text{reactor}})^{0.67}$	[16]
Storage tank	$C_{\text{tank}} = 167.2\times V_{\text{tank}}$	[17]
	$C_{\text{tank\_solid}} = V_{\text{tank}}\times C_{\text{steel}}$	[18]
Condenser, evaporator, heat exchanger, pump	$C_{Com} = C^0_p F_{Com} = C^0_p\,(B_1 + B_2 F_M F_P)$ $\log(C^0_p) = K_1 + K_2 \log(X_j) + K_3\,[\log(X_j)]^2$ $\log(F_p) = C_1 + C_2 \log(P_j) + K_3\,[\log(P_j)]^2$ $C_{\text{total}} = \sum_j (C_{com})_j \frac{\text{CEPCI}_{2024}}{\text{CEPCI}_{2001}}$	[19][20], [20]

*Subscript *j* refers to different components, *X* is the size (area m^2), *P* is the component pressure.

Table 2. *Coefficients for component capital cost* [19]

Coefficient	Pump	Condenser/evaporator	Heat exchanger
K_1	3.3892	4.3247	4.3247
K_2	0.0536	−0.303	−0.3030
K_3	0.1538	0.1634	0.1634

C_1	−0.3935	0.03881	−0.0016
C_2	0.3957	−0.11272	−0.0063
C_3	−0.0023	0.08183	0.0123
B_1	1.89	1.63	1.63
B_2	1.35	1.66	1.66
F_M	1.0	1.35	1.35

The Levelized Cost of Heat is estimated by Eq. (13),

$$\mathrm{LCoH} = \frac{CAPEX + \sum_{t=0}^{N} \frac{(OC_t + MC_t)}{(1+i)^t}}{\sum_{t=0}^{N} \frac{(Q_t)}{(1+i)^t}} \quad (13)$$

$$OC_t = \left(\text{material}_{\text{price}} \times \text{total mass of solid bulk}\right) + \left(\text{waste heat}_{\text{price}} \times Q_{\text{total heat supplied}}\right) \quad (14)$$

$$MC_t = MC_{fraction} \times CAPEX \quad (15)$$

Where, *CAPEX* is the total capital cost of the system (includes all component), N is the total system lifetime, OC_t is the operation cost in year t, MC_t is the maintenance cost in yeat t, Q_t is the heat output in yeat t.

3. Results

This section first presents the results of the system for fixed design parameters for a dehydration pressure of 20 kPa and hydration pressure of 400 kPa. Later, a detailed parametric study is presented for varying dehydration pressure, hydration pressure, system capacity, material price and waste heat price, and finally sensitivity on the component cost to address the uncertainties on the component cost and impact on LCoH.

3.1. Base system result

The results of each component together with the design parameters are presented in the below subsections.

3.1.1 Reactors

Table 3, presents the results and design parameters of both dehydration and hydration reactor. The dehydration reactor has an equilibrium temperature of 430 °C, whereas the hydration reactor has an equilibrium temperature of 590 °C, estimated using the Samms and Evans correlation. In order to initiate the dehydration reaction, the dehydration reactor is assumed to be operated at 440 °C, slightly higher than the dehydration equilibrium temperature. In contrast, the hydration reactor operates at 580 °C, slightly lower than the hydration equilibrium temperature to release heat. The system is designed to utilize 2.0 MW of waste heat as the input for the dehydration reaction. During operation, the hydration reaction releases an equal amount of heat, making the system thermally balanced and assuming negligible heat loss during the reaction. To achieve the heat output of 2 MW per cycle, the required amount of calcium hydroxide is estimated to be approximately 5256 kg. Based on this, the volume of the reactor is estimated to be 7.96 m^3. Finally, The COP_h of the system is evaluated to be around 0.61, representing the ratio of useful heat delivered (hydration output) to the heat input (dehydration + evaporator + superheater).

Table 3. *Result and design parameters of the dehydration and hydration reactors*

Parameter	Unit	value
Volume of reactor	m^3	7.96
Equillibrium temperature dehydration	°C	430
Equilibrium temperature hydration	°C	590
Dehydration reactor temperature	°C	440
Hydration reactor temperature	°C	580
$\dot{Q}_{\text{waste heat}}$	MW	2.0
$\dot{Q}_{\text{dehydration reaction}}$	MW	2.0
$\dot{Q}_{\text{hydration reaction}}$	MW	2.0
Mass of $Ca(OH)_2$	Kg	5256

3.1.2 Condenser and Precooler

The result and design parameters of condenser and precooler is listed below. It was assumed that the heat exchanged from the condenser and precooler is transferred to District heating (distribution network). The overall heat transfer coefficient for fluid-fluid medium is assumed to be 1000-4000 (W/m^2.K) [21]. The heat transfer rate of condenser and precooler is estimated as 0.84 MW and 0.27 MW and corresponding total heat exchanger area of condenser is estimated to be of ≈46.0 m^2 and precooler is of ≈1.90 m^2.

3.1.3 Evaporator and Superheater

The result and design parameters of evaporator and superheater is listed below. It was assumed that the heat of vaporization for water and the required superheat is transferred from the external heat transfer fluid (industrial waste heat). The overall heat transfer coefficient for gas-fluid medium is assumed to be 250 (W/m^2.K) [21]. The heat transfer rate of evaporator and superheater is estimated as 0.94 MW and 0.33 MW and corresponding total heat exchanger area of evaporator is estimated to be of ≈60.5 m^2, and superheater to be of ≈26.4 m^2.

3.1.6 Pump

Similarly, the result and design parameters of pump is listed below. The efficiency of the pump is assumed as 0.785 [12]. Overall, the net power required to increase the pressure of water from ambient to hydration pressure is found to be around 0.135 kW.

3.1.7 Economic result

Figure 2, shows the *CAPEX* and LCoH cost breakdown of the total system. From plot (a) it is evident that the reactor is the largest cost contributor, accounting for 39 % of the total cost. The material cost is the second largest contributor at around 28 %, followed by condenser and evaporator also making significant contributions. Moreover, the combined cost of heat exchangers represents nearly 30 % of the total system cost, indicating the major role in overall economics. On the other hand, pump and storage tanks contribute only a small fraction to the overall cost. Plot (b) shows the LCoH individual cost breakdown. From the economic analysis the levelized cost of heat of the system is estimated as 7.71 c€/kWh. Of which, the operation cost (material cost + waste heat cost) accounts for around 90 % of the LCoH, followed by *CAPEX* of around 6% and maintenance cost of around 4 %. Thus, the operational cost is the main driver influencing the levelized cost of heat.

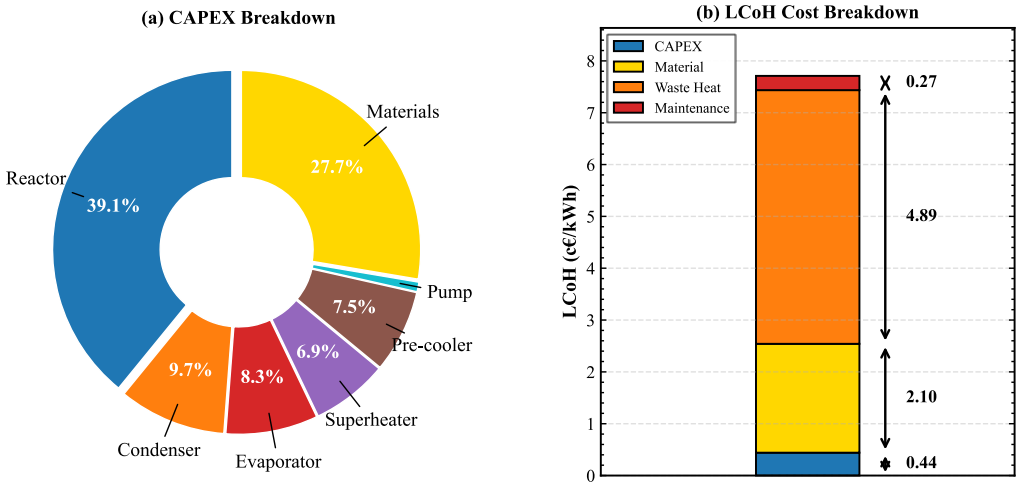

Figure 2. *Cost breakdown (a)CAPEX breakdown, (b) LCoH cost breakdown*

3.2. Parametric study

In addition to the techno-economic study of the base case system, a detailed parametric study has been conducted on the system design parameters such as dehydration pressure, hydration pressure, material price, waste heat price, and its effects on the temperature, heat transfer area, and LCoH has been studied.

3.2.1. Effect of dehydration and hydration pressure on reactor temperature

Figure 3, shows the reactor temperature and corresponding equilibrium temperature for both the dehydration and hydration reactors over a range of dehydration pressures (10–90 kPa) and hydration pressures (100–600

kPa). For the dehydration reaction to proceed, the solid bulk temperature must be higher than the equilibrium temperature and vice versa for hydration reactor. The result indicates that depending on the operating pressures the system can function either as heat storage or heat upgrading system. For example, at a dehydration pressure of 30 kPa and hydration pressure of 300 kPa, the dehydration reactor temperature is around ≈460 °C and equilibrium temperature is around ≈450 °C, while the hydration temperature is around ≈560 °C with equilibrium temperature of ≈570 °C, operating at the given pressure range enables the system to store and release heat at higher temperatures. For the base case system, with a dehydration pressure of 20 kPa and hydration pressure of 400 kPa, the system operates as heat upgrading system with a temperature lift of 140 °C. However, it is important to note that operating at very low or very high pressures can impact the LCoH and will be discussed in the following subsections.

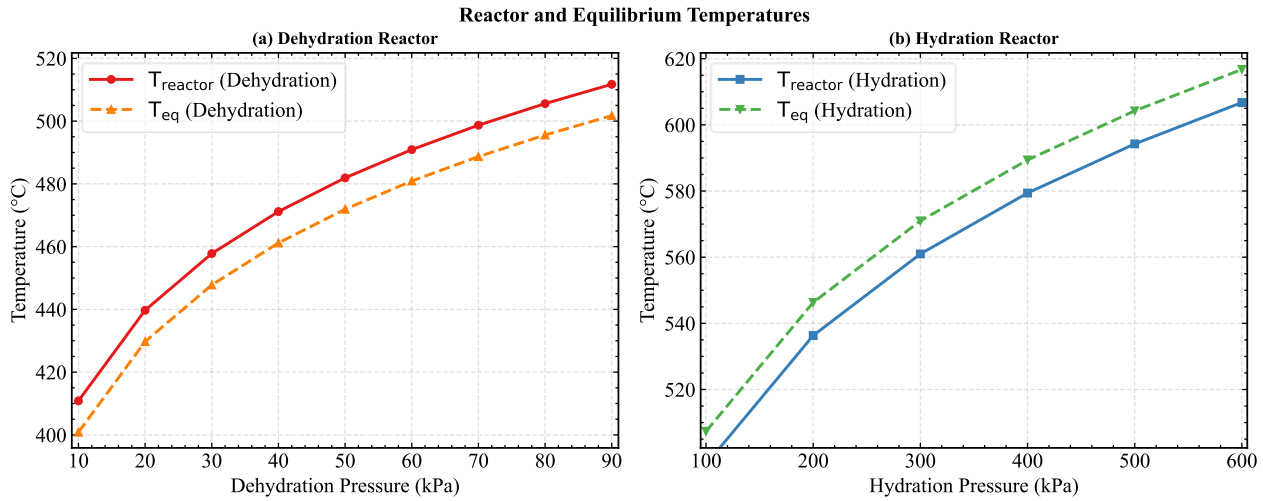

Figure 3. *Parametric study of dehydration and hydration pressure on the reactor and equilibrium temperature*

3.2.2. Effect of dehydration pressure

This parametric study shows the effect of dehydration pressure on the LCoH of the system and heat exchanger area of the system components across a wide pressure range of 10–90 kPa and for a fixed hydration pressure of 400 kPa.

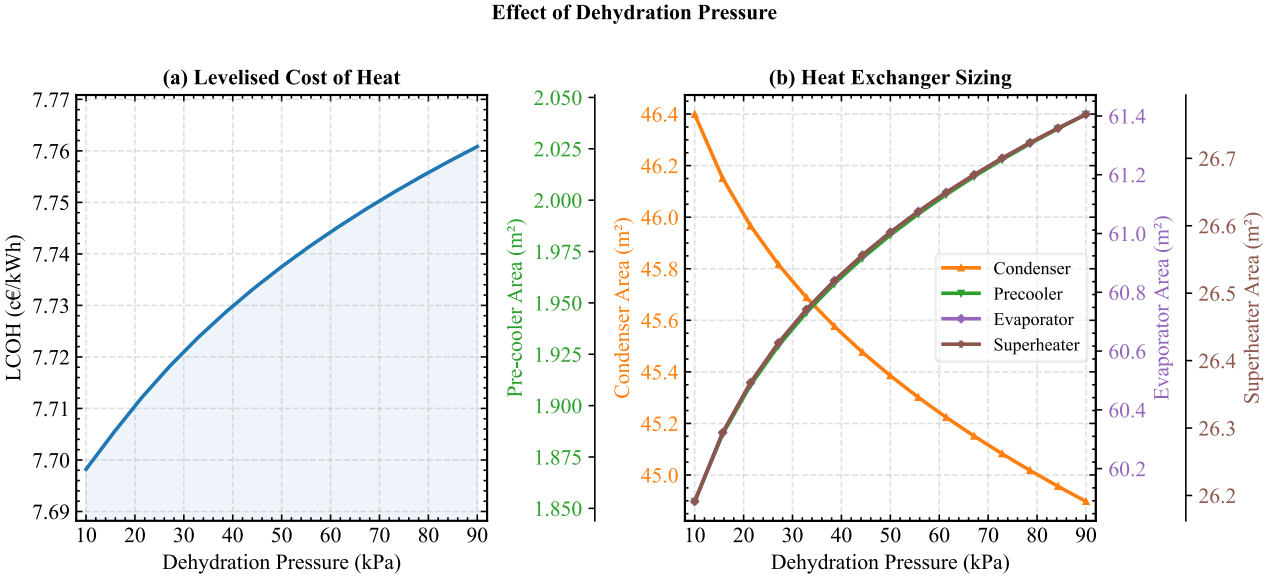

Figure 4*. Parametric study of dehydration pressure on (a) Levelized Cost of Heat, and (b) heat exchanger sizing requirements*

From the plot (a) in Figure 4, a minimal increase in the LCoH is observed of around 7.70 – 7.76 c€/kWh across the entire pressure range, indicating that variations in dehydration pressure have a negligible impact on the overall economic performance of the system. In contrast, plot (b) shows a slight decrease in the condenser area of about 3% for dehydration pressure from 10-90 kPa. Subsequently, the evaporator, superheater, and

pre-cooler exhibit only marginal increase in area over the same range. The decrease in area of condenser is due to, at higher dehydration pressure the enthalpy of vaporization of water decreases, therefore the heat transfer rate is decreased and due to which the area decreases. On contrary, the increase in area for evaporator and superheater is due to the decrease in enthalpy of reaction of the solid material at higher pressures and therefore increases the mass flow rate of water. As the mass flow of water is constant throughout the system, therefore for increase in mass flow rate at higher pressures increases the heat transfer rate of evaporator, and superheater and thus increase in area is observed. In addition, only a small variations in the heat exchangers area are observed and is due to the heat transfer rate of the heat exchanger and fixed overall heat transfer coefficients, which constrains the variations in heat transfer area. As the change in heat transfer rate is only minimal of around 3 % for the $\dot{Q}_{\text{condenser}}$, 2 % for the $\dot{Q}_{\text{evaporator}}$, 20 % for the $\dot{Q}_{\text{precooler}}$, and around 2 % for the $\dot{Q}_{\text{superheater}}$ for the variation in dehydration pressure from 10-90 kPa respectively.

The fact that dehydration pressure has minimal effect on the LCoH is because increase in dehydration pressure affects the equipment size and that increases the *CAPEX* of the system, but the operational cost is the main driver influencing the levelized cost of heat than the *CAPEX*, which remains relatively constant across the entire pressure range. As a result, the LCoH remains largely unaffected.

3.2.3. Effect of hydration pressure

This parametric study shows the effect of hydration pressure on the LCoH of the system and heat exchanger area of the system components across a wide pressure range of 100–600 kPa and for fixed dehydration pressure of 20 kPa.

Similar to Figure 4, from Figure 5, it is evident that hydration pressure has very little effect on both the levelized cost of heat and the size of components. As shown in plot (a), the levelized cost of heat increases slightly from 7.62 – 7.74 c€/kWh across the entire range of hydration pressures. This suggests that variations in hydration pressure does not significantly affect the economic performance of the system.

Whereas, in Plot (b), the change in heat exchangers area for evaporator and superheater is noted. The condenser and precooler remain unchanged as these components are independent of the hydration pressure. The condenser area remains constant at around 46 m² and the pre-cooler at around 1.9 m². A small change in area of superheater is observed of about 23 m² to 28 m², increasing roughly by 22%. Whereas the evaporator exhibits only a marginal increase from 59 to 61 m². However, the small changes in component sizes lead to only minimal changes in capital cost as observed in section 3.2.2.

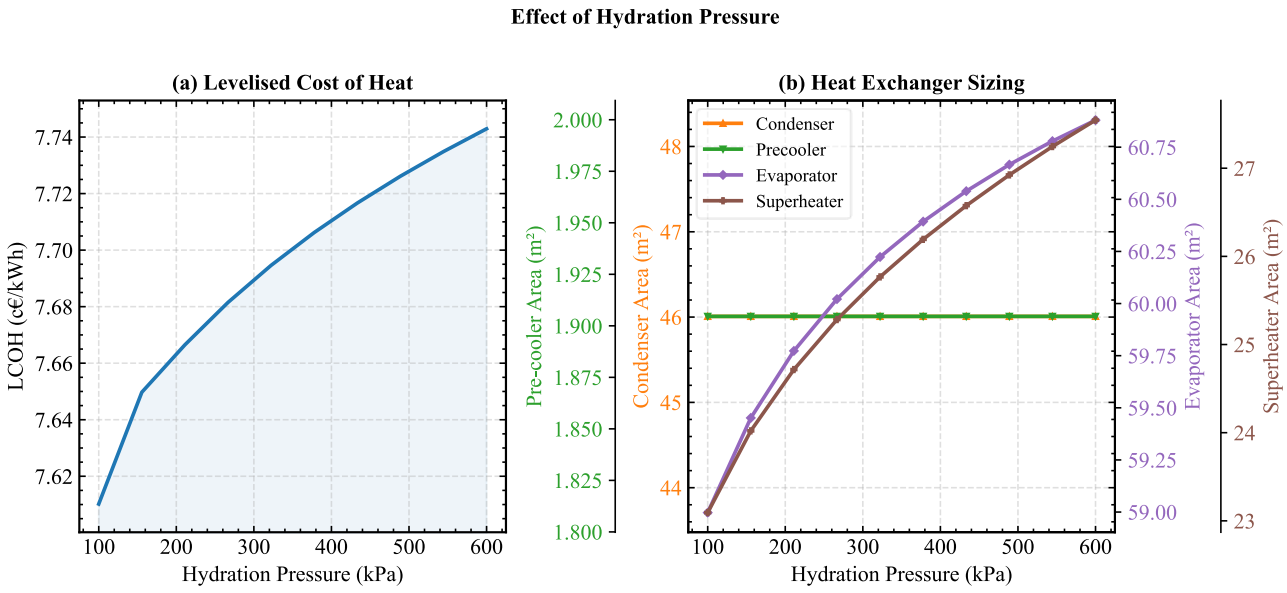

Figure 5. *Parametric study of hydration pressure on (a) Levelized Cost of Heat, and (b) heat exchanger sizing requirements*

3.2.4. Effect of System capacity

Figure 6, shows the effect of system capacity on the LCoH and heat exchanger area. From the plot (a) it is evident that the system capacity has a significant influence on the levelized cost of heat, the LCoH decreases from approximately 9.0 c€/kWh to 7.17 c€/kWh for system capacity of 0.5 MW to 50 MW respectively, corresponding to an overall reduction of 20 %. The decrease in LCoH is more evident in capacities between

0.5 and 10 MW, the LCoH drops sharply by from 9.0 to 7.32 c€/kWh. Beyond this range, the LCoH remains almost constant, with only a marginal reduction of around 2% observed between 10 to 50 MW. It is due to the scaling behaviour of cost and heat output. The capital cost increase with the system size not only but also the required amount of waste heat and the total mass of material to deliver the required heat output, which increases the operational cost which is around 6 time higher than *CAPEX* for a system capacity of 0.5 MW, 16 times higher for system capacity of 2 MW (base case), and 60 times higher for system capacity of 50 MW. As a result, the LCOH decreases rapidly at smaller scales due to increase in ratio of energy delivered to the total system cost,but approaches a plateau at higher capacities indicates that the ratio of energy delivered, and total system cost where almost constant and constrain further cost reductions.

Plot (b) shows that the heat exchanger areas scale proportionally with system capacity. The evaporator area increases from around 15 m² at 0.5 MW to 1500 m² at 50 MW, while the condenser increases from ≈11 m² to ≈1200 m², and the superheater from around 6.5 m² to 700 m². In contrast, the pre-cooler remains relatively small, staying below 50 m² across the entire capacity range, and therefore does not represent a limiting factor for scaling this is due to the chosen technical design constraints of the precooler. Overall, these results suggest that a capacity range of approximately 10–20 MW provides a practical balance between capital cost efficiency and LCOH reduction.

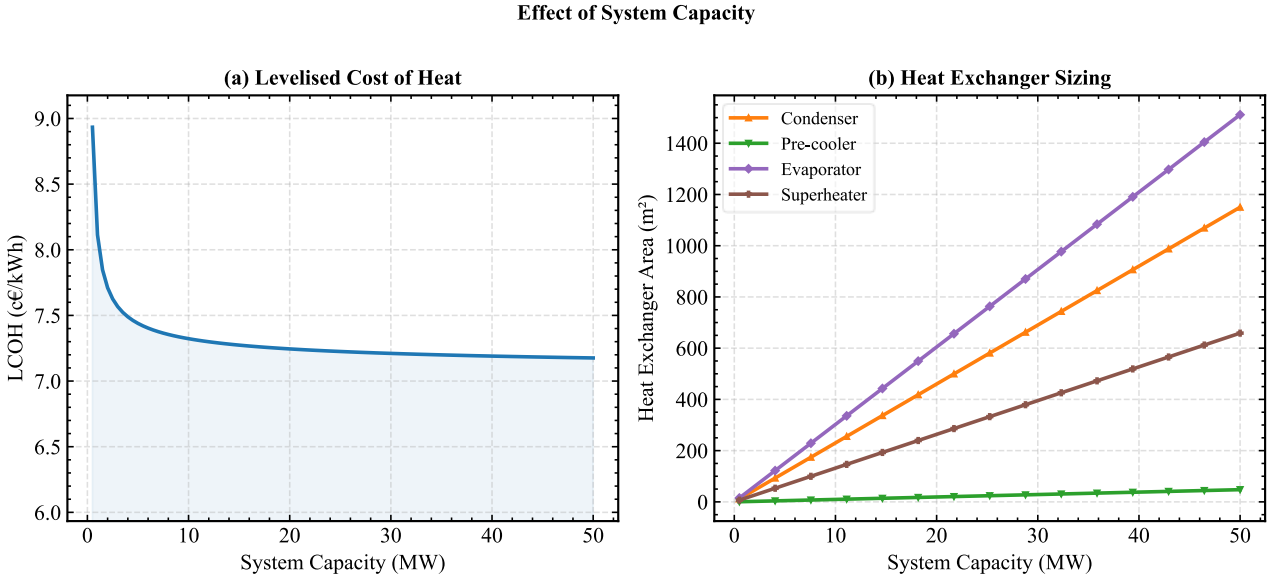

Figure 6. *Parametric study of system capacity on (a) Levelized Cost of Heat, and (b) heat exchanger sizing requirements*

3.2.5. Effect of Material price and Waste heat price

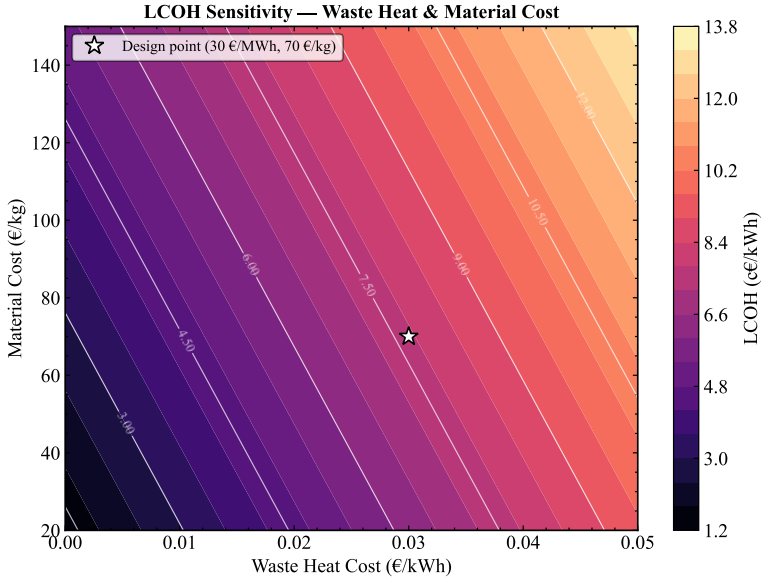

Figure 7. *Sensitivity analysis of material price and waste heat price on levelized cost of heat*

The influence of waste heat price and material price on the levelized cost of heat is shown in Figure 7. For the analysis the waste heat price is increases from 0-0.05 €/kWh, and the material price is increased from 20-150 €/kg. It is observed that LCoH is much more sensitive to the price of waste heat than to the material price. When waste heat is free and material price is at 20 €/kg, LCoH reaches its minimum of about 1.2 c€/kWh, but it rises to around 14 c€/kWh at a waste heat price of 0.05 €/kWh and material price of 150 €/kg. This is because waste heat represents the main energy input and the largest operational cost in the system.

The design point (0.03 €/kWh waste heat and 70 €/kg material) results in an LCoH of about 7.71 c€/kWh, which is in the range of the reported LCoH values for hydration heat transformer (2-7.5 c€/kWh) [12], high-temperature industrial heat pumps (4.2 c€/kWh) [23], and with conventional natural gas boilers (7.35 c€/kWh) [24]. Thus, from the plot it is evident that free waste heat is critical for economic viability. Therefore, systems located near industries such as refineries, cement plants, or iron and steel plant - where waste heat is available at low cost can achieve LCoH values below 3–4 c€/kWh, making the system highly competitive.

3.2.6. Sensitivity study on the component cost of the system

Figure 8, shows the effect of varying the cost of individual components on the LCoH. The green shaded region (−100% to 0%) represents cost reduction scenarios, while the red shaded region (0% to +100%) represents cost increase scenarios. From the plot it is evident that the reactor exhibits the highest sensitivity, with LCoH ranging from 7.9 to 7.51 c€/kWh. With a maximum increase of around 2.5 % from the base case LCoH, followed by condenser and evaporator of around 1.1 % increase from the base case LCoH respectively. Other components have minimal effect on the LCoH for the given range. Overall, the results suggest that system costs can be minimized by improvements in reactors and heat exchangers. However, the potential economic gains from such improvements remain limited, as operation costs constitute the dominant share of the total system cost and are largely insensitive to design modifications.

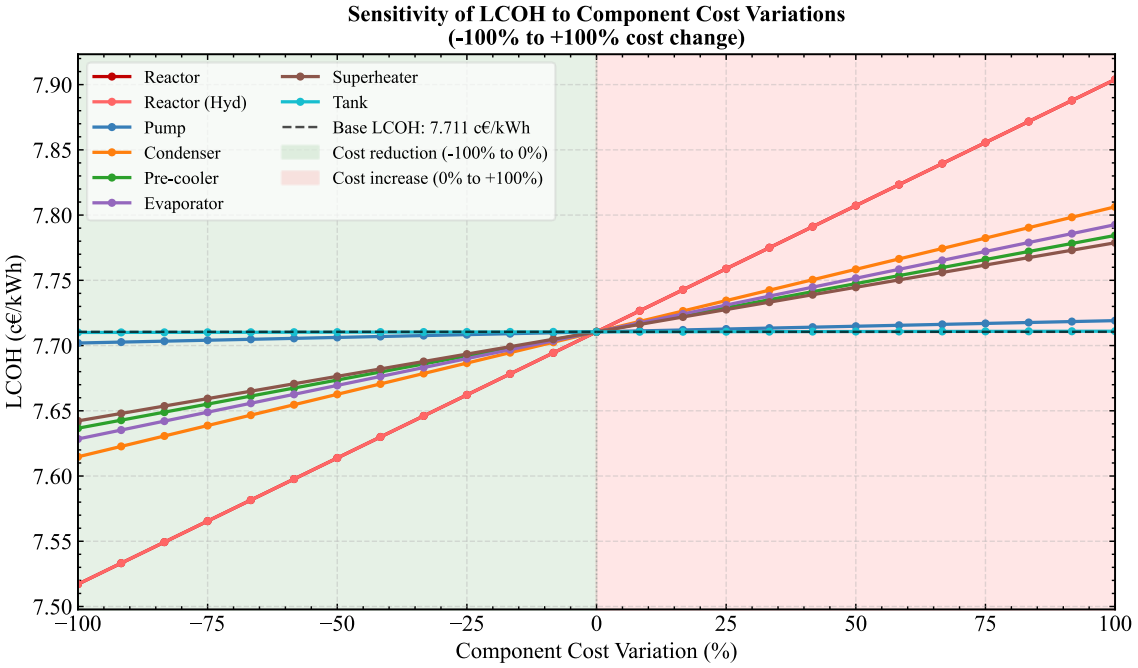

Figure 8. *Sensitivity of levelized cost of heat to component cost variation*

4. Discussion

In the present analysis, several assumptions have been made that may influence the accuracy of the results. The sensible heat required for preheating of material has not taken into account in the analysis. Furthermore, the reactor cost function is based on correlations developed for packed bed reactors, whereas a moving bed reactor is used in the current system. Although both reactor exhibit similar functional behavior in terms of solid–gas interaction and heat transfer, differences in design, reaction kinetics, operating condition may increase the capital cost. The analysis assumes complete conversion, neglecting the effects of reaction rates, and temperature-dependent kinetics, as these factors can significantly influence reactor performance, residence time, and overall system efficiency. A constant heat transfer coefficient (*U*-value) has been assumed for all heat exchangers based on the heat transfer medium. A more accurate estimation would require the use of Nusselt number correlations to capture flow regime and geometry effects.

5. Conclusion

Overall, the following conclusions were drawn for the the proposed Thermochemical heat upgrade system:

- The reactor is the single largest cost contributor (39 %), with heat exchangers collectively accounting for nearly 30 % of total system cost. The base case LCoH is estimated at 7.71 c€/kWh.
- Varying dehydration pressure from 10–90 kPa has a minimal effect on LCoH, which remains nearly constant at ≈7.5 c€/kWh. Heat exchanger areas change only marginally (e.g., a 3% decrease in condenser area), resulting that dehydration pressure is not a sensitive economic parameter. Similarly, hydration pressure (100–600 kPa) has very little effect on LCoH, though the superheater area increases by ~22 % (from 23 to 28 m²). Overall, variations in hydration pressure do not significantly influence the system's economic performance.
- System capacity has a significant influence, reducing LCoH by 20% from 9.0 c€/kWh (0.5 MW) to 7.17 c€/kWh (50 MW). With the heat exchanger areas scale proportionally.Overall, a system capacity of 10–20 MW capacity offering the optimal balance between cost efficiency and LCoH reduction.
- LCoH is highly sensitive to waste heat cost than the material price. At free waste heat and low material cost (20 €/kg), LCoH drops to 1.2 c€/kWh, whereas at 0.05 €/kWh waste heat and 150 €/kg material, it rises to ≈14 c€/kWh, proving that free or low-cost waste heat is critical for economic viability and competitiveness.
- The dehydration and hydration reactors are the most sensitive components, causing up to a ±5 % change in LCoH (from 7.23 to 8.02 c€/kWh). However, potential economic gains from design improvements are limited, as operation costs dominate the total system cost and remain largely unaffected by such modifications.

Acknowledgments

This work has been carried out in the framework of the European Union's Horizon Europe research and innovation program under grant agreement No. 101192888 (STOREDGE).

Nomenclature

U	Heat transfer coefficient, W/(m^2 K)
$\dot{m}$	Mass flow rate, kg/s
$\mathrm{COP_h}$	Coefficient of Performance for heating, -
LCoH	Levelized Cost of Heat, c€/kWh
$\dot{\mathrm{Q}}$	Heat transferred rate, W
T_{reactor}	Reactor temperature, °C
V_{reactor}	Volume of reactor, m^3
CAPEX	Capital cost, €
OC	Operating cost, €
MC	Maintenance cost, €

Greek symbols

ΔH	Reaction enthalpy, (J/mol)
ρ	Density, (kg/m^3)

Subscripts and superscripts

t	year
eq	equilibrium

References

[1] IEA (2021), Net Zero by 2050, IEA, Paris https://www.iea.org/reports/net-zero-by-2050.

[2] IEA, World Energy Balances, IEA, Paris https://www.iea.org/data-and-statistics/data-product/world-energy-balances

[3] Schaube, F., Koch, L., Wörner, A., & Müller-Steinhagen, H. (2012). A thermodynamic and kinetic study of the de- and rehydration of $Ca(OH)_2$ at high H_2O partial pressures for thermo-chemical heat storage. Thermochimica Acta, 538, 9–20. https://doi.org/10.1016/j.tca.2012.03.003

[4] Pardo, P., Deydier, A., Anxionnaz-Minvielle, Z., Rougé, S., Cabassud, M., & Cognet, P. (2014). A review on high temperature thermochemical heat energy storage. Renewable and Sustainable Energy Reviews, 32, 591–610.https://doi.org/10.1016/j.rser.2013.12.014

[5] Schmidt, M., Szczukowski, C., Roßkopf, C., Linder, M., & Wörner, A. (2014). Experimental results of a 10 kW high temperature thermochemical storage reactor based on calcium hydroxide. Applied Thermal Engineering, 62(2), 553–559. https://doi.org/10.1016/j.applthermaleng.2013.09.020

[6] Cosquillo Mejia, A., Afflerbach, S., Linder, M., & Schmidt, M. (2020). Experimental analysis of encapsulated CaO/$Ca(OH)_2$ granules as thermochemical storage in a novel moving bed reactor. Applied Thermal Engineering, 169, 114961. https://doi.org/10.1016/j.applthermaleng.2020.114961

[7] Wang, W., Yang, J., Guene Lougou, B., Huang, Y., & Shuai, Y. (2024). Effect of fluid direction and reactor structure on heat storage performance of $Ca(OH)_2$/CaO based on shell-tube thermochemical energy storage device. Renewable Energy, 234, 121249. https://doi.org/10.1016/j.renene.2024.121249

[8] Jia, Y., Wang, Y., Zhou, X., Xu, Y., Liu, M., Ling, H., & Chen, H. (2025). Critical review of CaO/$Ca(OH)_2$ thermochemical energy storage material. Renewable and Sustainable Energy Reviews, 216, 115678. https://doi.org/10.1016/j.rser.2025.115678

[9] Michalski, S., Hanak, D. P., & Manovic, V. (2019). Techno-economic feasibility assessment of calcium looping combustion using commercial technology appraisal tools. *Journal of Cleaner Production, 219*, 540–551.https://doi.org/10.1016/j.jclepro.2019.02.049

[10] Carro, A., Chacartegui, R., Ortiz, C., & Becerra, J. A. (2022). Analysis of a thermochemical energy storage system based on the reversible $Ca(OH)_2$/CaO reaction. *Energy, 261*, 125064. https://doi.org/10.1016/j.energy.2022.125064

[11] Vecchi, A., & Sciacovelli, A. (2023). Long-duration thermo-mechanical energy storage – Present and future techno-economic competitiveness. *Applied Energy, 334*, 120628. https://doi.org/10.1016/j.apenergy.2022.120628

[12] Rahbari, H. R., & Arabkoohsar, A. (2025). Hydration heat transformer: A groundbreaking technology for sustainable process heating. *Energy, 337*, 138757. https://doi.org/10.1016/j.energy.2025.138757

[13] Samms, J.A.C. and Evans, B.E. (1968), Thermal dissociation of Ca(OH)2 at elevated pressures. J. Appl. Chem., 18: 5-8. https://doi.org/10.1002/jctb.5010180102

[14] Wang, M., Chen, L., He, P., & Tao, W.-Q. (2019). Numerical study and enhancement of $Ca(OH)_2$/CaO dehydration process with porous channels embedded in reactors. *Energy, 181*, 417–428.https://doi.org/10.1016/j.energy.2019.05.184

[15] Wang, M., Chen, L., Zhou, Y., & Tao, W.-Q. (2022). Numerical simulation of the calcium hydroxide/calcium oxide system dehydration reaction in a shell-tube reactor. *Applied Energy, 312*, 118778. https://doi.org/10.1016/j.apenergy.2022.118778

[16] Li, W., Markides, C. N., Zeng, M., & Peng, J. (2024). 4E evaluations of salt hydrate-based solar thermochemical heat transformer system used for domestic hot water production. *Energy, 286*, 129602. https://doi.org/10.1016/j.energy.2023.129602

[17] Fan, R., & Xi, H. (2022). Energy, exergy, economic (3E) analysis, optimization and comparison of different Carnot battery systems for energy storage. *Energy Conversion and Management, 252*, 115037. https://doi.org/10.1016/j.enconman.2021.115037

[18] Martínez Castilla, G., Guío-Pérez, D. C., Johnsson, F., & Pallarès, D. (2024). Techno-economics of solids-based thermochemical energy storage systems for large scale, high-temperature applications. *Journal of Energy Storage, 101*, 113944. https://doi.org/10.1016/j.est.2024.113944

[19] Turton R, Bailie R, Whiting W, Shaeiwitz J. Analysis, SynthesisDesign Chem Process 2008.

[20] The Chemical Engineering Plant Cost Index ® - Chem Eng n.d https://www.chemengonline.com/pci-home

[21] Kakaç, S., Liu, H., & Pramuanjaroenkij, A. (2002). *Heat exchangers: Selection, rating, and thermal design* (2nd ed.). Taylor & Francis.

[22] Romanov, D., Chakraborty, I., & Holler, S. (2025). Comparative analysis of scenarios of data center waste heat utilization for district heating networks of different generations. *Energy Conversion and Management, 334*, 119856. https://doi.org/10.1016/j.enconman.2025.119856

[23] IEA (2022), *The Future of Heat Pumps*, IEA, Paris https://www.iea.org/reports/the-future-of-heat-pumps, Licence: CC BY 4.0

[24] IEA (2025), *Can low-temperature heat in factories be electrified competitively?*, IEA, Paris https://www.iea.org/commentaries/can-low-temperature-heat-in-factories-be-electrified-competitively, Licence: CC BY 4.0

[25] Thermo Fisher Scientific. *Calcium hydroxide, 98%, extra pure*. https://www.thermofisher.com/order/catalog/product/219180010 [accessed 2026-03-14].